symmetry

MDPI

Article

An Enhanced Calculation Method of the Heat Rejection System of a Free-Piston Stirling Engine (FPSE) Operating on the Moon

Sergey Smirnov [1], Mikhail Sinkevich [1,2], Yuri Antipov [1], Igor Tsarkov [3], Sergei Kupreev [1] and Hassan Khalife [1,3,*]

[1] Academy of Engineering, Peoples' Friendship University of Russia (RUDN University), 6 Miklukho-Maklaya Str., 117198 Moscow, Russia; smirnov-sv@rudn.ru (S.S.); sinkevich-mv@rudn.ru (M.S.); antipov-yua@rudn.ru (Y.A.); kupreev-sa@rudn.ru (S.K.)
[2] Gas Turbine Technologies Laboratory, Joint Institute for High Temperatures, Russian Academy of Sciences, 13 2 Izhorskaya Str., 125412 Moscow, Russia
[3] Nauka Power Technology LLC, 42 1 Bolshoy Boulevard, 121205 Moscow, Russia; ia.tsarkov@evogress.com
* Correspondence: hassan.khalife.rudn@gmail.com

Abstract: In this paper, an enhanced calculation method of a heat rejection system operating on the moon is presented. This was taken into consideration in the developed calculation method and in the propagation of heat fluxes with the radiation of the removed heat. The developed method made it possible to effectively evaluate the capabilities of various refrigerants and choose the radiator parameters and the refrigerant flow regime in a less time-consuming process and with minimal deviations (<5%) compared to the previously developed two-dimensional radiator model by the authors. A comparative analysis was carried out for two refrigerants: helium and liquid ammonia. It has been established that when using liquid ammonia, there are more possibilities for varying the geometric parameters of the radiator. The use of liquid ammonia as a refrigerant made it possible to reduce the power spent on pumping the refrigerant through the radiator. Using helium, the power for pumping the refrigerant was $N_R = 5.1$ W during a turbulent flow $Re = 4500$. On the other hand, the power for pumping liquid ammonia was $N_R = 0.27$ W. In addition, using liquid ammonia increased the heat flux radiated by the radiator pipe by 3.9 times, which made it to possible to increase the fin width and reduce the length of the radiator pipe.

Keywords: moon colonization; lunar power plant; free-piston Stirling engine; radiator; heat rejection; space exploration

Citation: Smirnov, S.; Sinkevich, M.; Antipov, Y.; Tsarkov, I.; Kupreev, S.; Khalife, H. An Enhanced Calculation Method of the Heat Rejection System of a Free-Piston Stirling Engine (FPSE) Operating on the Moon. *Symmetry* **2022**, *14*, 1168. https://doi.org/10.3390/sym14061168

Academic Editor: Yury Razoumny

Received: 3 April 2022
Accepted: 1 June 2022
Published: 6 June 2022

1. Introduction

Mankind has always been interested in space exploration. Providing a highly reliable power system plays a critical role in the success of space missions. The space missions of this era are evolving to a whole new level, which includes the colonization of new planets and the construction of bases with a permanent presence of humans. The first mission on the list of modern space missions is the colonization of the Moon. Russia, USA, China, Japan and other countries are planning to build a base on the Moon within the next 15–20 years [1–3].

The discovery of water at the Moon's poles about 10 years ago and the possibility of extracting rare earth gases such as helium 3 (a non-radioactive isotope) revived interest in the Moon. In addition, it is believed that the colonization of the Moon will provide people a useful experience in preparation for the exploration of Mars. Lunar bases will have high power requirements to support activities such as scientific experiments, mining and processing, astronomical observations and surface exploration. Therefore, providing a reliable source of energy at these bases is considered extremely important.

A key component of space nuclear power systems is the prime mover, which converts thermal energy into electrical energy. Among the well-known nuclear converters with a

high potential for application in space missions is the free-piston Stirling engine (FPSE). In July 2018, NASA acknowledged the FPSE as the most reliable heat engine in the history of civilization. The FPSE unit began operation in the Glenn research center in 2002 and has been operating continuously for more than 14 years without any signs of degradation [4].

Due to the extremely low temperatures and harsh environmental conditions in space, the heat rejection process is considered to be quite complex and implies high demands on the design. Therefore, designing a highly efficient heat rejection system is crucial for the nominal performance and maximum efficiency of the power generation system. Heat rejection systems for space nuclear power systems should be coordinated with the thermodynamic cycles of the power plants in such a way as to maximize the performance of the space nuclear power system while maintaining the specific mass of the heat rejection system and the total specific gravity of the power generation system (kg/kW) to a minimum [5].

Several heat rejection systems have been implemented in space, one of which is widely used—the fluid loop system. This system transfers heat from the equipment, in our case the power generation system, to the radiators, which then rejects the heat into free space. This system can be a mechanically pumped single-phase circuit or a two-phase heat pipe circuit.

Heat pipes have the significant advantage of being completely passive with no moving parts, making them exceptionally suitable for use in space. A heat pipe is a thin hollow pipe filled with a liquid appropriate for the temperature range in which it is intended to operate. At the hot end, the liquid is in the vapor phase and tries to fill the pipe by passing through the pipe to the cold end, where it gradually condenses into the liquid phase. The walls of the pipe, or corresponding channels cut into the pipe, are filled with wick material which returns the liquid by surface tension to the hot end where it is re-evaporated and recirculated. Heat pipes are most commonly used because of their lightness and high thermal conductivity.

Currently, heat pipes are often used for the thermal control of spacecrafts. The heat pipe evaporator is mounted on the components that need to be cooled, and the condenser is mounted on the heatsink panel to dissipate heat. However, heat pipes have a number of limitations compared to a mechanically pumped loop heat rejection system. These limitations are mainly related to the amount of heat rejected and the flexibility of heat transfer control.

On the other hand, the mechanically pumped loop heat rejection system ensures efficient transfer of large amounts of heat at a controlled heat transfer rate and operating temperature. Several works discuss mechanically pumped single-phase liquid loop heat rejection systems and their potential for future space missions. In one study [6], the experimental and analytical results of a heat rejection system consisting of a single-phase mechanically pumped loop and a space radiator are presented. The prototype was developed for future crewed exploration missions to provide a large amount of heat dissipation capability. In [7], a study on refrigerant selection for a high-temperature mechanically pumped fluid loop for space applications is presented; it describes the trade study used to select the high-temperature working fluid for the system and the initial development testing of loop components. In [8], a mini mechanically pumped loop designed for the thermal control of small satellites is presented. In [9,10], a highly self-adaptive cold plate for the single-phase mechanically pumped fluid loop for spacecraft thermal management and hybrid system are studied.

In addition to mechanically pumped single-phase liquid loop systems, heat pipes are also actively being studied. In [11], a heat rejection technology based on heat pipes for space application is presented, where the feasibility of the proposed model is described. In [12], a titanium–water heat pipe radiator for the thermal management of space fission power systems, such as the Kilopower system, is studied. The testing results demonstrated that the developed radiator is able to transfer the required power at the working temperature of 400 K under space-like testing conditions. In [13], a space power system consisting of FPSEs based on potassium heat pipes is presented. In [14,15], sodium variable conductance heat pipes with a Carbon–Carbon radiator for radioisotope Stirling systems are studied.

The active research and development of heat rejection systems for space applications confirms the importance of the studies conducted in this paper. In mathematical modeling, the symmetry of the distribution of heat fluxes as a result of heat conduction along the radiator fins from the radiator pipes and radiation heat flows from two symmetrical surfaces of the radiator was taken into account. In this work, we consider a mechanically pumped single-phase heat rejection system, which is a continuation of our previous work [16]. The calculation method in our previous work took into account the influence of uneven temperature distribution over the surface of the radiator, variable speed and temperature of the refrigerant in the radiator pipes. This is considered crucial while designing a radiator for space applications. However, the main design parameters of the radiator based on the choice of the refrigerant were determined using a time-consuming iterative process, which is discussed in detail in the work itself.

The authors have continued research in this area and developed an enhanced calculation method of a heat rejection system operating on the moon, which allows the time to be decreased for determining the main design parameters of the radiator and the most effective refrigerant. The enhanced method made it possible to effectively evaluate the capabilities of various refrigerants and choose the radiator parameters and the refrigerant flow regime. This was possible by deriving formulas based on acceptable assumptions, which are explained in detail in the next section. In addition, a comparative analysis is presented for two refrigerants: helium and liquid ammonia. It is important to note that the calculation method is not limited to a specific type of refrigerant. Any refrigerant can be considered in the calculation method; however, the operating range of the refrigerant should meet the requirements of the heat rejection system. The refrigerant operating temperature and pressure ranges before encountering a phase change, thermal capacity, thermal conductivity and viscosity should be taken into consideration when choosing a refrigerant.

Helium and liquid ammonia were considered in this work due to their attractive thermophysical properties and suitable operational conditions for the considered FPSE heat rejection system. In a previously published work of the authors, a detailed comparative study of several refrigerants was presented [17]. Helium gas is known for its high heat-transfer capabilities, one of the main reasons it is used as the working fluid inside the FPSE. On the other hand, the choice of liquid ammonia as a refrigerant is due to its proven advantages in space thermal management systems. Advantages of ammonia include: high thermal capacity, wide range of operating temperatures, low weight when compared to water and its viscosity which leads to minimum pumping power through pipes. The International Space Station's (ISS) active thermal control systems include a liquid-ammonia coolant loop along the station's main truss which keeps the station's electricity-generating solar panels cool [18].

This work is organized as follows: First, an overview of the lunar power plant proposed is described. Second, the main steps of the enhanced calculation method are presented. The dependences of the change in the geometrical parameters of the radiator on the thermodynamic properties of the refrigerant and the flow regime are established. Then, the calculation results are presented. An example of selecting the dimensions of a radiator with a given specific radiation flux per unit area using helium and liquid ammonia is presented. Finally, the conclusions are provided.

2. Materials and Methods

A detailed description of the heat rejection system of the FPSE operating on the Moon has already been presented in one of the published works of the authors [19]. However, it is also presented in this work to give the reader a better understanding of the calculation method and the results presented in this work. An overview diagram of the FPSE and the heat rejection system is shown in Figure 1. The engine model considered in this work was developed by Microgen Engine Corporation and is the same model implemented by Nauka-Power Technology LLC in its autonomous off-grid power solutions for hard to

reach and remote facilities which require a reliable source of power [20,21]. This particular FPSE model has a high potential for application in future space missions.

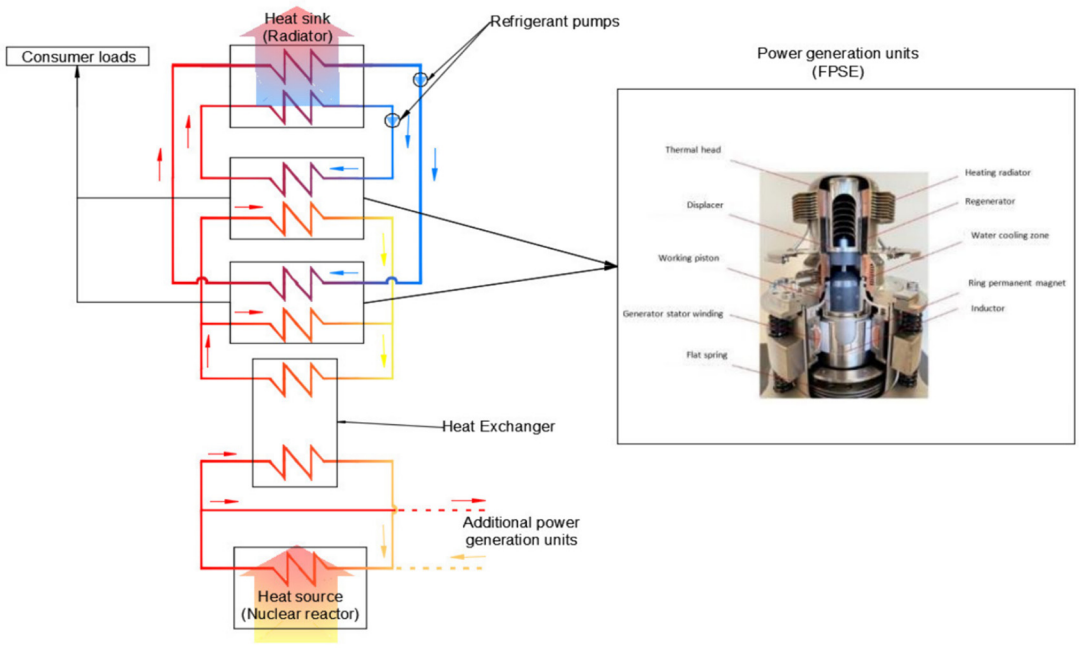

Figure 1. Overview scheme of the lunar power plant.

The proposed power plant considers supplying heat from the nuclear reactor to the FPSE. The FPSE has two main moving parts: the displacer and the working piston. Both operate in a closed helium environment and are not mechanically coupled to each other. Helium shuttles from the expansion zone (heater) to the compression zone (cooler) due to the temperature difference and cyclical movements of the displacer and power piston. Between the expansion and compression zones there is a porous heat regenerator, which increases the efficiency of the cooling and heat processes of the helium shuttling between the zones. The mechanical energy of the reciprocating movement of the working piston is transformed into electrical energy through a single-phase synchronous linear generator, the inductor of which with permanent magnets is connected to the working piston. Several FPSEs can be powered by the nuclear reactor in the system, however, for convenience, only one FPSE was considered in this paper.

The FPSE is a combination of heat exchangers: a heater, a regenerator and a cooler, which form an internal circuit. In the cooler, heat is rejected from the helium to the outer circuit. The outer circuit (heat rejection system) consists of a pump and a radiator, in which a refrigerant circulates. The heat transferred from the internal circuit to the outer circuit is rejected into free space by the radiator.

Structurally, the radiator is a set of radiant panels operating according to a parallel scheme of inclusion in the radiator's hydraulic path, connected together by a system of inlet and outlet collectors. The structural form of the radiating panel can be made in the form of parallel pipes, to which the fins are rigidly attached [22]. In this work, two options for the radiator were considered (Figure 2), in which the diameter of the pipes is smaller (option 1) or greater (option 2) than the thickness of the radiator fin. Each radiator pipe has two fins for radiating heat into free space: one from the left side and another from the right side. The fins are symmetric with respect to the pipe. Appendix A provides more detailed information about the design features of the radiator options.

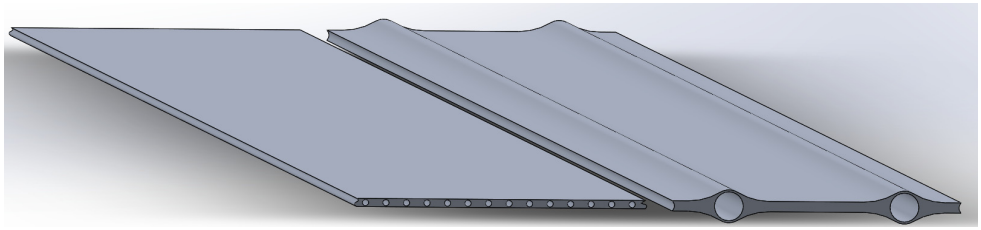

Figure 2. Two options of the radiator design.

The heat transfer processes occurring in the outer circuit (heat rejection system) are convective heat transfer (q_{conv}) and radiation (q_{rad}). Convective heat transfer occurs in the radiator pipes while the refrigerant is passing through them. Heat is transferred from the refrigerant to the pipes' walls. Afterwards, heat is radiated from the radiator surface into free space [23,24]. Considering the two heat transfer processes occurring, the following condition must be satisfied:

$$q_L = q_{rad} = q_{conv} \tag{1}$$

$$q_L = \frac{q_s}{n_p} \tag{2}$$

To calculate the radiator, we must specify the total heat flux that must be rejected (q_s); temperature at the inlet and outlet of the radiator pipe (T_{in}; T_{out}); and the thermodynamic parameters of the refrigerant (μ_{in}; μ_{out}; ρ_{in}; ρ_{out}; h_{in}; h_{out}; λ).

Next, the total flow of the refrigerant through the radiator is determined:

$$G_s = \frac{q_s}{\Delta h_L} \tag{3}$$

where the change in stagnation enthalpy through one pipe:

$$\Delta h_L = h_{in} - h_{out} \tag{4}$$

Through one radiator pipe, the refrigerant mass flow is as follows:

$$G_{ref} = \frac{G_s}{n_p} \tag{5}$$

The refrigerant mass flow must be constant and is determined as follows:

$$G_{ref} = \rho_{in} \cdot w_{in} \cdot \frac{\pi \cdot d^2}{4} \tag{6}$$

Heat q_l transferred as a result of convection:

$$q_{conv} = \alpha \cdot S_t \cdot (T_h - T_w) \tag{7}$$

where the surface area for heat transfer:

$$S_t = \pi \cdot d \cdot L_R \tag{8}$$

The heat transferred to the walls of the radiator pipe is further distributed along the fins of the radiator by thermal conduction and then the heat is rejected by radiation from the surface of the radiator q_R:

$$q_R = \sigma \cdot \varepsilon \cdot F_R \cdot (T_w^4 - T_S^4) \tag{9}$$

where the radiation area:

$$F_R = 2 \cdot L_R \cdot B_R \tag{10}$$

It is worth noting that the radiation is considered from two surfaces of the radiator. Detailed information about the calculation of the width of one section of the radiation surface B_R and the total width of the radiator B_C is given in Appendix A.

Based on the condition of heat balance ($q_{conv} = q_R$), the thermal state of the radiator fin was determined. As already mentioned, the enhanced calculation method of the heat rejection system allows the time to be decreased for determining the main design parameters of the radiator and the most effective refrigerant. The enhanced calculation method is carried out in two stages:

1. Preliminary calculation to determine the main geometric parameters of the radiator based on the refrigerant chosen using derived formula.
2. Calculation of the radiator based on the result of the preliminary calculations. At this stage, the calculation is carried out using the previously developed method which takes into consideration the uneven distribution of temperatures over the surface of the radiator, variable speed and temperature of the refrigerant inside the pipe. The method for determining the temperature state of the radiator in a two-dimensional formulation is described in detail in the work [19].

The amount of heat radiated from the surfaces of the radiator fins at a constant ambient temperature is determined by the surface area and the temperature level in the radiator fins. Moreover, in formula (9), the temperatures are to the fourth power $(T_R^4 - T_S^4)$; therefore, the greater the difference between the surface temperature T_R and ambient temperature T_S, the more efficient the heat rejection. At a given ambient temperature T_S, the specific heat flux per unit area q_F depends on the fin surface temperature T_R.

For the preliminary calculations, it was assumed that the temperature of the fin is constant and equal to the temperature of the inner surface of the pipe ($T_R = T_w$), and the temperature of the refrigerant in the pipe is equal to the average temperature:

$$T_m = \frac{T_{in} + T_{out}}{2} \tag{11}$$

Subsequent studies have shown the validity of this assumption. A temperature difference coefficient for convective heat transfer $K_T = \frac{T_w}{T_h}$ is introduced for convenience. The closer the wall temperature T_w to the refrigerant temperature T_h, the greater the temperature difference between the radiator fin T_R and the ambient temperature T_S; therefore, the greater the heat flux that will be rejected per unit area q_F. Theoretically, the minimum total radiator area for heat rejection of a given heat flux q_s will be when $T_R = T_h$:

$$F_{Ramin} = \frac{q_s}{\sigma \cdot \varepsilon \cdot (T_h^4 - T_S^4)} \tag{12}$$

Then, the maximum heat flux emitted from the radiator surface:

$$q_{Fmax} = \frac{q_s}{F_{Ramin}} = \sigma \cdot \varepsilon \cdot (T_h^4 - T_S^4) \tag{13}$$

According to these formulas, it is possible to determine the limiting values of the radiator area and heat flux for evaluating the results obtained. In practice, it is impossible to achieve them, since a temperature difference is necessary for the heat rejection process, therefore $T_h > T_w$ and $K_T < 1.0$.

The total area of the radiation surface of the radiator is as follows:

$$F_{Ra} = 2 \cdot L_R \cdot B_{Ra} = 2 \cdot L_R \cdot B_R \cdot n_p \tag{14}$$

$$F_{Ra} = \frac{q_s}{\sigma \cdot \varepsilon \cdot (T_w^4 - T_S^4)} \tag{15}$$

A formula for determining the pipe diameter d for a given mean Reynolds number Re_m is derived. The Reynolds number of the refrigerant at the pipe inlet can be determined as follows:

$$Re_{in} = \frac{2 \cdot Re_m}{\frac{\mu_{in}}{\mu_{out}} + 1} \tag{16}$$

and

$$Re_{in} = \frac{w_{in} \cdot d}{\nu_{in}} \tag{17}$$

Further, we perform rearrangement of the formulas:

$$w_{in} \cdot d = Re_{in} \cdot \nu_{in} \tag{18}$$

The total flow rate G_S is found from the formulas (5) and (6):

$$G_S = \rho_{in} \cdot w_{in} \cdot \frac{\pi \cdot d^2}{4} \cdot n_p \tag{19}$$

Substituting (18) into (19):

$$G_S = \rho_{in} \cdot \frac{\pi}{4} \cdot n_p \cdot Re_{in} \cdot \nu_{in} \cdot d \tag{20}$$

Considering:

$$\mu_{in} = \rho_{in} \cdot \nu_{in} \tag{21}$$

and

$$\mu_v = \frac{\mu_{in} + \mu_{out}}{\mu_{in} \cdot \mu_{out}} \tag{22}$$

We obtain a formula showing the relationship between the pipe diameter and the number of radiator pipes:

$$d \cdot n_p = \frac{2 \cdot G_S \cdot \mu_v}{\pi \cdot Re_m} \tag{23}$$

Or considering formula (3), we obtain:

$$d \cdot n_p = \frac{2 \cdot q_s \cdot \mu_v}{\pi \cdot \Delta h_L \cdot Re_m} \tag{24}$$

We combine all the parameters of the initial data for calculation in this formula and introduce a coefficient for convenience:

$$A_1 = \frac{2 \cdot q_s \cdot \mu_v}{\pi \cdot \Delta h_L} \tag{25}$$

We obtain:

$$d \cdot n_p = \frac{A_1}{Re_m} \tag{26}$$

For a given number of pipes, the formula for calculating the diameter of the radiator pipe is as follows:

$$d = \frac{A_1}{n_p \cdot Re_m} \tag{27}$$

It is possible to set the diameter of the radiator pipe and determine the number of pipes:

$$n_p = \frac{A_1}{d \cdot Re_m} \tag{28}$$

In this case, the number of pipes must be an integer. This can be achieved by appropriate adjustment of the diameter d. Then, we derive the formula for calculating the width of one section of the radiation surface from ($q_{rad} = q_{conv}$) and ($\alpha \cdot d = Nu \cdot \lambda$):

$$B_R = \frac{\pi}{2 \cdot \sigma \cdot \varepsilon} \cdot \frac{T_h \cdot (1 - K_T)}{(K_T \cdot T_h)^4 - T_S^4} \cdot \lambda \cdot Nu \tag{29}$$

A necessary condition (check Appendix A) in this case is:

$$B_S > d + 2 \cdot t \tag{30}$$

The thickness of the pipe (t) is chosen based on the strength calculation of the structure. The total width of the radiator was calculated as follows:

$$B_{Ra} = B_R \cdot n_p \tag{31}$$

Ceteris paribus, setting the coefficient K_T or wall temperature $T_w = T_h \cdot K_T$, we can determine the width of the radiator fin B_R, providing the temperature difference ($\Delta T = T_h - T_w$). When specifying the number of radiator pipes, we define:

1. Radiation surface area:

$$F_R = \frac{q_s}{\sigma \cdot \varepsilon \cdot n_p \cdot (T_w^4 - T_S^4)} \tag{32}$$

2. Radiator pipe length:

$$L_R = \frac{F_R}{2 \cdot B_R} \tag{33}$$

The formula for determining the length of the radiator can be obtained by substituting into formula (33): the formulas for determining the radiator's radiation area F_R (32); width of the radiation surface for one fin section B_R (29); and number of pipes n_p (28):

$$L_R = \frac{d}{2} \cdot \frac{1}{T_h \cdot (1 - K_T)} \cdot \frac{\Delta h_L \cdot Re_m}{\mu_v \cdot \lambda \cdot Nu} \tag{34}$$

3. Specific heat flux of radiator surface:

$$q_F = \frac{q_s}{F_R \cdot n_p} = \frac{q_s}{F_{Ra}} = \sigma \cdot \varepsilon \cdot (T_w^4 - T_S^4) \tag{35}$$

The total radiation area of the radiator F_{Ra} and the specific heat flux q_F, taking into account the assumptions made for a given heat flux q_s and ambient temperature T_s, depends on the pipe wall temperature T_w and coefficient of temperature difference K_T. The dimensional formulas B_R and L_R are determined by the number of pipes n_p, pipe diameter d, thermodynamic parameters of the refrigerant and flow regime Re.

Another important factor for evaluating the efficiency of a radiator design is the power spent on pumping the refrigerant through the radiator. By changing the number of radiator pipes, it is possible to achieve the required geometric dimensions with acceptable power losses for pumping the refrigerant through the radiator. The calculation of the hydraulic resistance inside the radiator was carried out using the following method.

The power spent on pumping the refrigerant through the radiator was calculated as follows:

$$N_R = \frac{G_s \cdot \Delta P_R}{\eta \cdot \rho_h} \tag{36}$$

The Darcy friction factor for laminar flow:

$$f = \frac{64}{Re_m} \tag{37}$$

For turbulent flow:

$$f = [0.79ln(\frac{Re_m}{8})]^{-2} \tag{38}$$

The pressure drop was calculated as follows:

$$\Delta P_R = f\frac{L_R}{d}\cdot\frac{\rho_h \cdot {w_h}^2}{2} \tag{39}$$

Rearranging:

$$N_R = \frac{G_s \cdot f}{\eta}\cdot\frac{L_R}{d}\cdot\frac{{w_h}^2}{2} \tag{40}$$

Considering that the refrigerant velocity:

$$w_h = \frac{Re_m \cdot \nu_m}{d} \tag{41}$$

We obtain:

$$N_R = \frac{G_s \cdot f}{\eta}\cdot\frac{L_R}{d^3}\cdot\frac{{Re_m}^2 \cdot {\nu_m}^2}{2} \tag{42}$$

For a laminar flow, this formula can be rearranged, taking into account formula (37):

$$N_R = \frac{32 \cdot G_s \cdot {\nu_m}^2}{\eta}\cdot\frac{L_R}{d^3}\cdot Re_m \tag{43}$$

or

$$N_R = A_{N_R}\cdot\frac{L_R}{d^3}\cdot Re_m \tag{44}$$

where the pumping power coefficient:

$$A_{N_R} = \frac{32 \cdot G_s \cdot {\nu_m}^2}{\eta} \tag{45}$$

An increase in the pipe length L_R and a decrease in the pipe diameter d lead to an increase in the power for pumping the refrigerant. The pipe length L_R depends on the diameter d (34), and the diameter d is related to the number of pipes n_p (28).

The formulas include the Nusselt number Nu and Reynolds Re, which characterize the features of heat transfer and refrigerant flow [24,25].

1. Nusselt number for laminar flow when $\frac{Pe \cdot d}{L_R} < 100$:

$$Nu = 3.66 \tag{46}$$

where Peclet number:

$$Pe = Re \cdot Pr \tag{47}$$

2. Transitional flow from laminar to turbulent when $2300 \leq Re < 4000$:
For the condition $0.5 < Pr < 1.5$:

$$Nu = 0.0214\left(Re^{0.8} - 100\right)Pr^{0.4}[1 + (\frac{d}{L_R})^{\frac{2}{3}}] \tag{48}$$

For the condition $1.5 < Pr < 500$:

$$Nu = 0.012\left(Re^{0.87} - 280\right)Pr^{0.4}[1 + (\frac{d}{L_R})^{\frac{2}{3}}] \tag{49}$$

3. Nusselt number for turbulent flow:

$$Nu = \frac{\frac{f}{8} \cdot Re \cdot Pr}{R_1 + R_2\sqrt{\frac{f}{8}}(Pr^n - 1)} \tag{50}$$

where Prandtl number:

$$Pr = \frac{\gamma}{a} \tag{51}$$

$$R_1 = 1, R_2 = 12.7, n = \frac{2}{3} \tag{52}$$

The above formulas made it possible to study the influence of the flow regime on the geometrical parameters of the radiator and the power spent on pumping the refrigerant depending on the given specific heat flux emitted by the radiator for various refrigerants.

Based on the studies carried out, the main design parameters of the radiator can be preliminarily determined (d; B_R; L_R; n_p). After conducting the preliminary calculation using the above formulas, the obtained results are refined using the previously developed calculation method of the radiator (two-dimensional model), which takes into account the uneven distribution of temperatures over the area of the radiator fin [19].

To compare two refrigerants with the same initial data (q_s; T_{in}/T_{out}; ΔT), the following formulas are proposed (subscripts 1 and 2 are used to indicate the refrigerant):

1. From formula (24), we obtain:

$$\frac{d_1 \cdot n_{p1}}{d_2 \cdot n_{p2}} = \frac{\mu_{v1} \cdot \Delta h_{L2} \cdot Re_{m2}}{\mu_{v2} \cdot \Delta h_{L1} \cdot Re_{m1}} \tag{53}$$

For flows with the same mean value of Reynolds number Re_m:

$$\frac{d_1 \cdot n_{p1}}{d_2 \cdot n_{p2}} = \frac{\mu_{v1} \cdot \Delta h_{L2}}{\mu_{v2} \cdot \Delta h_{L1}} \tag{54}$$

or

$$\frac{d_1 \cdot n_{p1}}{d_2 \cdot n_{p2}} = \frac{K_\mu}{K_h} \tag{55}$$

where the viscosity and enthalpy ratios:

$$K_\mu = \frac{\mu_{v1}}{\mu_{v2}}; K_h = \frac{\Delta h_{L1}}{\Delta h_{L2}} \tag{56}$$

2. From formula (29):

$$\frac{B_{R1}}{B_{R2}} = \frac{\lambda_1 \cdot Nu_1}{\lambda_2 \cdot Nu_2} = \frac{B_{R1}}{B_{R2}} = K_\lambda \cdot \frac{Nu_1}{Nu_2} \tag{57}$$

where the radiation surface ratio:

$$K_\lambda = \frac{\lambda_1}{\lambda_2} \tag{58}$$

3. From formula (34):

$$\frac{L_{R1}}{L_{R2}} = \frac{d_1 \cdot \lambda_2 \cdot Nu_2}{d_2 \cdot \lambda_1 \cdot Nu_1} \cdot \frac{\mu_{v2} \cdot \Delta h_{L1} \cdot Re_{m1}}{\mu_{v1} \cdot \Delta h_{L2} \cdot Re_{m2}} \tag{59}$$

4. Total required radiation surface, an important parameter for evaluating the heat rejection efficiency of the refrigerant:

$$S_{ta} = S_t \cdot n_p = q_s \cdot d \cdot \frac{1}{T_h \cdot (1 - K_T)} \cdot \frac{1}{\lambda \cdot Nu} \tag{60}$$

$$\frac{d_1 \cdot n_{p1}}{d_2 \cdot n_{p2}} = \frac{\mu_{v1} \cdot \Delta h_{L2} \cdot Re_{m2}}{\mu_{v2} \cdot \Delta h_{L1} \cdot Re_{m1}} \quad (61)$$

$$\frac{S_{ta1}}{S_{ta2}} = \frac{d_1 \cdot \lambda_2 \cdot Nu_2}{d_2 \cdot \lambda_1 \cdot Nu_1} \quad (62)$$

For laminar flows ($\frac{Pe \cdot d}{L_R} < 100$; $Nu = 3.66$), the formulas are simplified:

$$\frac{B_{R1}}{B_{R2}} = K_\lambda \quad (63)$$

$$\frac{S_{ta1}}{S_{ta2}} = \frac{d_1 \cdot \lambda_2}{d_2 \cdot \lambda_1} = \frac{d_1}{d_2} \cdot \frac{1}{K_\lambda} \quad (64)$$

$$\frac{L_{R1}}{L_{R2}} = \frac{d_1 \cdot Re_{m1}}{d_2 \cdot Re_{m2}} \cdot \frac{K_h}{K_\lambda \cdot K_\mu} \quad (65)$$

For flows with the same mean value of Reynolds number Re_m:

$$\frac{L_{R1}}{L_{R2}} = \frac{d_1}{d_2} \cdot \frac{K_h}{K_\lambda \cdot K_\mu} \quad (66)$$

3. Results and Discussion

The initial data for calculating the radiator are:

a. The FPSE parameters:
   i. The amount of heat that must be rejected from the working fluid in the FPSE;
   ii. The minimum temperature of the working fluid at the cold side of the FPSE.
b. The refrigerant used in the heat rejection system; thermodynamic properties.
c. Ambient temperature.

The ambient temperature in this study is of great importance due to its direct influence on the efficiency of the heat rejection process. Temperatures on the Moon are extreme. Ranges of temperature changes relative to their location on the Moon and a parametric study of the energy systems of the lunar base can be found in [26,27]. The location of the lunar power plant considered in this work was at one of the poles, where the maximum ambient temperature reaches 200 K (−73 °C), which is considered the most suitable for lunar bases according to several space agencies. At lower ambient temperatures, the difference between the temperature of the fins and the ambient temperature increases, resulting in an increase in the efficiency of heat rejection.

Helium and liquid ammonia were considered as refrigerants; their main properties (gas constant, enthalpy, heat capacity *Cp*, dynamic viscosity, thermal conductivity) were set according to the data from these works [28,29]. The main parameters of the FPSE considered in the calculation are shown in Table 1.

Table 1. The main parameters of the FPSE.

Parameter	Value	Unit
Output Power	1100	W
Total thermal power	3600	W
Amount of heat to be rejected	2500	W
Efficiency	30	%
Maximum cycle temperature	600	°C
Minimum cycle temperature	50	°C

To compare the efficiency of refrigerants, the following conditions were set constant:

- The heat flow that must be rejected in the radiator from the FPSE $q_s = 2500$ W;

- Refrigerant temperatures at the inlet and outlet of the radiator pipe T_{in}/T_{out} = 280/260 ($T_m = T_h = 270\ K$);
- Average pipe wall temperature $T_w = 269\ K$, consequently $K_T = \frac{T_w}{T_h} = 0.996$;
- Refrigerant pressure in the heat rejection loop system—1 MPa;
- Fin thickness h_R = 0.005 m.

If the specified temperature difference is provided as $\Delta T = T_h - T_w = 1\ K$, then the total radiation surface area of the radiator, regardless of the refrigerant used and the flow regime, will be constant (14): $F_{Ra} = 14.3\ m^2$.

Initially, helium was considered as a refrigerant for the calculation. During a laminar flow ($\frac{Pe \cdot d}{L_R} < 100$; Nu = 3.66) and based on the given initial data, the fin width remains constant (29) $B_S = B_R = 0.0052$ m (Option 1 in Appendix A).

When specifying the pipe diameter, the condition $B_S > d + 2 \cdot t$ must be taken into account. For the example under consideration, with a pipe diameter of 2.0 mm and a thickness t = 1.0 mm, the distance between two pipes b_{r1} is only 1.2 mm.

Depending on the considered pipe diameter, we determine the number of pipes n_p, pipe length L_R, as well as the total width of the radiator B_a and the power spent on pumping the refrigerant N_R for different flow rates Re. The results for a pipe of a diameter d = 2.0 mm are shown in Figures 3–5. With a decrease in the refrigerant flow rate, the number of pipes increases and, consequently, the total width of the radiator, while the length of the pipe and the pumping power decrease. During a transitional flow (2300 < Re < 4000), the value of the Nu number increases, the heat rejection from the refrigerant increases, which consequently affects the geometric dimensions of the radiator.

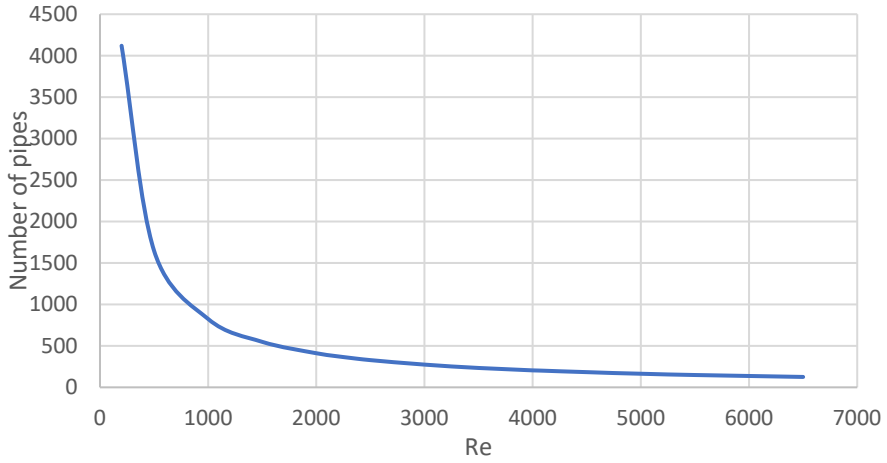

Figure 3. Dependence of the number of pipes on the Reynolds number (Refrigerant—He).

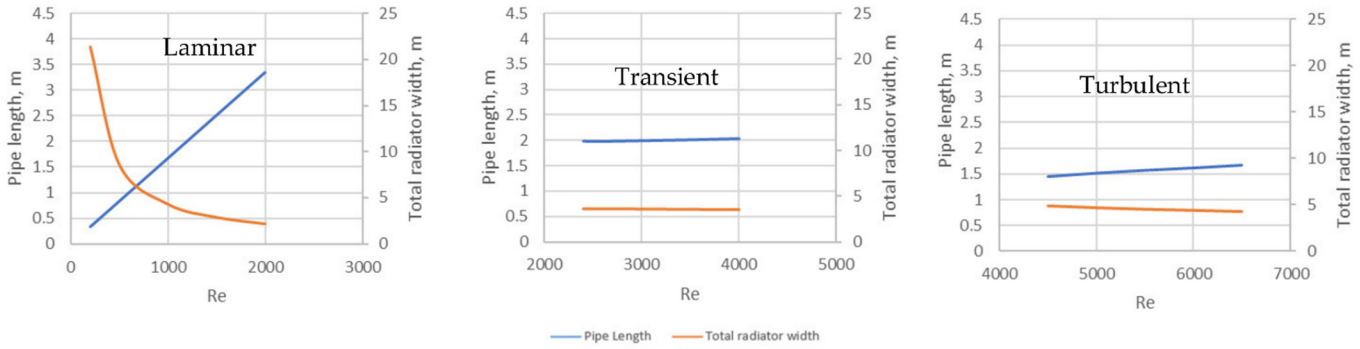

Figure 4. Dependence of the pipe length and the total width of the radiator on the flow regime (Refrigerant—He).

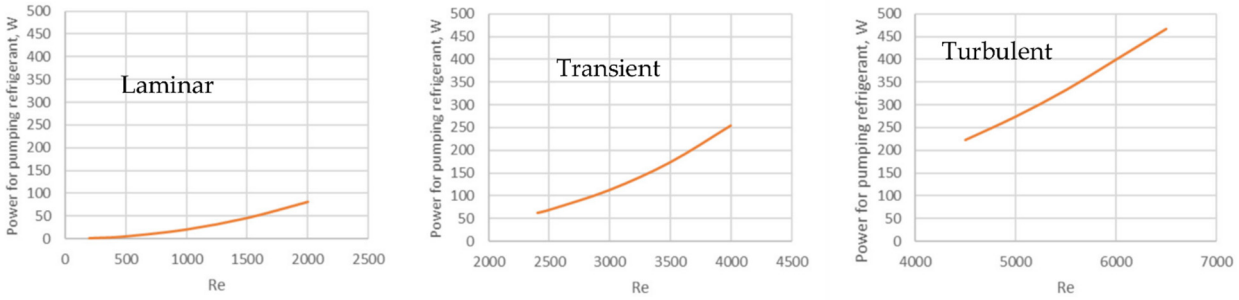

Figure 5. Dependence of the pumping power of the refrigerant through the radiator on the flow regime (Refrigerant—He).

For a pipe with a diameter $d = 2.0$ mm at $Re = 500$ $(B_R = 0.0052\ m)$, the following results were obtained:

- Number of pipes: $n_p = 1648$;
- Total width of the radiator: $B_C = B_{Ra} = 8.53\ m$;
- Pipe length: $L_R = 0.84\ m$;
- Power spent on pumping the refrigerant: $N_R = 5.1\ W$.

It is worth noting that with an increase in the number of pipes, the dimensions of the distribution collectors of the radiator increase. This would increase the total hydraulic losses at the inlet and outlet of the pipes.

During turbulent flows ($Re > 4000$), the heat transfer from the refrigerant to the pipe walls increases, therefore providing the required specific heat radiation flux per unit area, and the width of the fin increases.

For the same pipe diameter $d = 2.0$ mm at $Re = 4500 (B_R = 0.0268\ m)$, the following results were obtained:

- Number of pipes: $n_p = 183$;
- Total width of the radiator: $B_C = B_{Ra} = 4.91\ m$;
- Pipe length: $L_R = 1.45\ m$;
- Power spent on pumping the refrigerant: $N_R = 222.6\ W$.

Analyzing the results, it can be seen that the number of pipes decreased. However, the power required to pump the refrigerant through the radiator increased to a high value which is unacceptable. The design can be significantly improved by increasing the fin width of the radiator B_R, and increasing the pipe diameter d, which leads to minimizing the power required to pump the refrigerant N_R (Option 2 in Appendix A). For instance, the increase in diameter to $d = 10.8$ mm leads to the following results at $Re = 4500$:

- Number of pipes: $n_p = 34$;
- Total width of the radiator: $B_C = 0.81\ m$;
- Total width of the radiation surface: $B_{Ra} = 0.91\ m$;
- Pipe length: $L_R = 7.83\ m$;
- Power spent on pumping the refrigerant: $N_R = 7.7\ W$.

Similar calculations for liquid ammonia were carried out and the results were compared. During a laminar flow ($\frac{Pe \cdot d}{L_R} < 100$; $Nu = 3.66$) and based on the given initial data, the fin width remains constant $B_R = 0.0202\ m$. For the given initial data, $A_1 = 196.2$. The calculation results are shown in Figures 6–8.

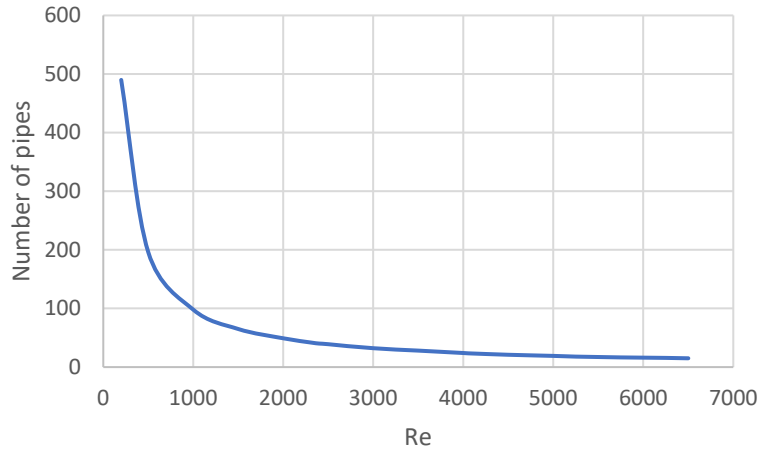

Figure 6. Dependence of the number of pipes on the Reynolds number (Refrigerant—NH_3).

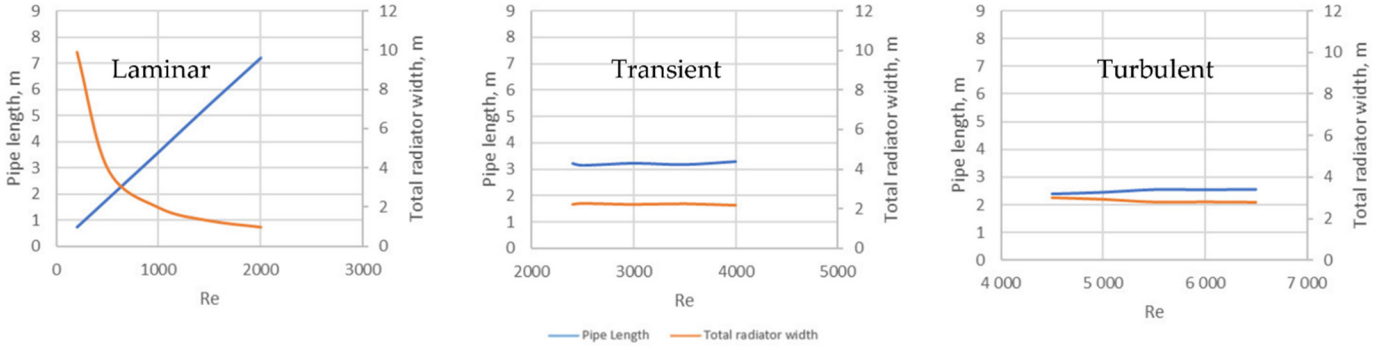

Figure 7. Dependence of the pipe length and the total width of the radiator on the flow regime (Refrigerant—NH_3).

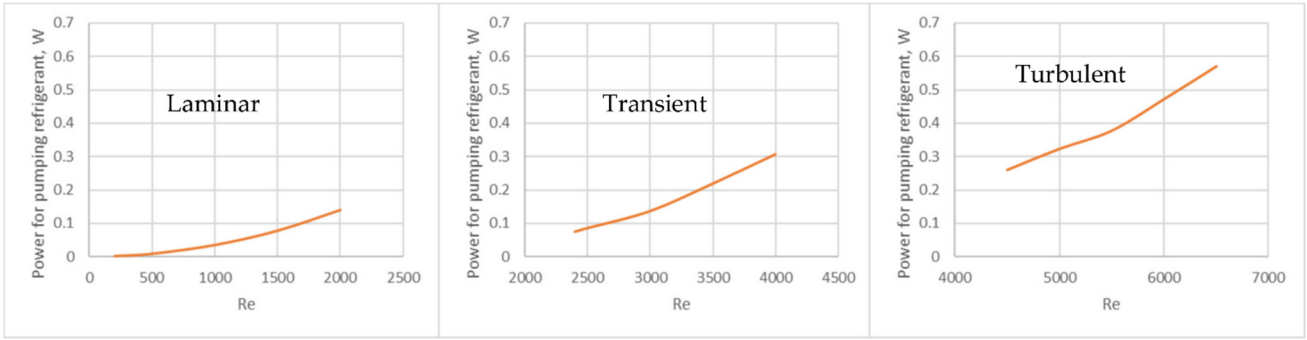

Figure 8. Dependence of the pumping power of the refrigerant through the radiator on the flow regime (Refrigerant—NH_3).

For a pipe with a diameter $d = 2.0$ mm at $Re = 500$, the following results were obtained:

- Number of pipes: $n_p = 196$;
- Total width of the radiator: $B_C = B_{Ra} = 3.97\ m$;
- Pipe length: $L_R = 1.8\ m$;
- Power spent on pumping the refrigerant: $N_R = 0.009\ W$.

During turbulent flows, the heat transfer from the refrigerant to the pipe walls increases. At $Re = 4500$, the fin width B_R increases ($B_R = 0.143\ m$). The fin width B_R allows the pipe diameter to increase.

The graphs of the dependences of the number of pipes n_p, pipe lengths L_R, as well as the total width of the radiation surface of the radiator B_{Ra}, and the power spent on pumping liquid ammonia N_R for various pipes diameters d at Re = 4500 are shown in Figures 9–11.

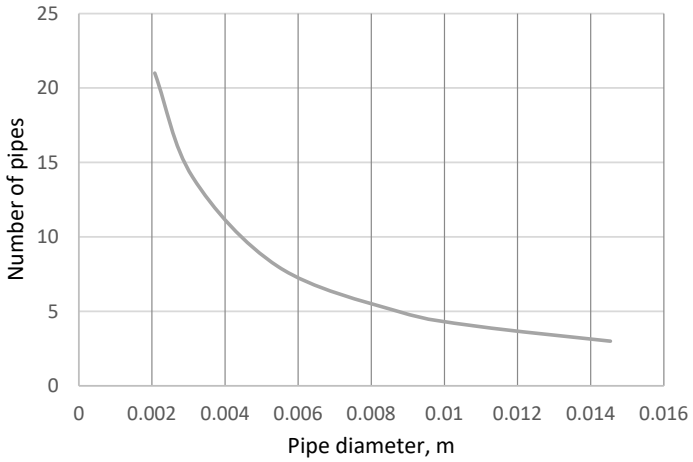

Figure 9. Dependence of the number of pipes on the pipe diameter (Refrigerant—NH_3).

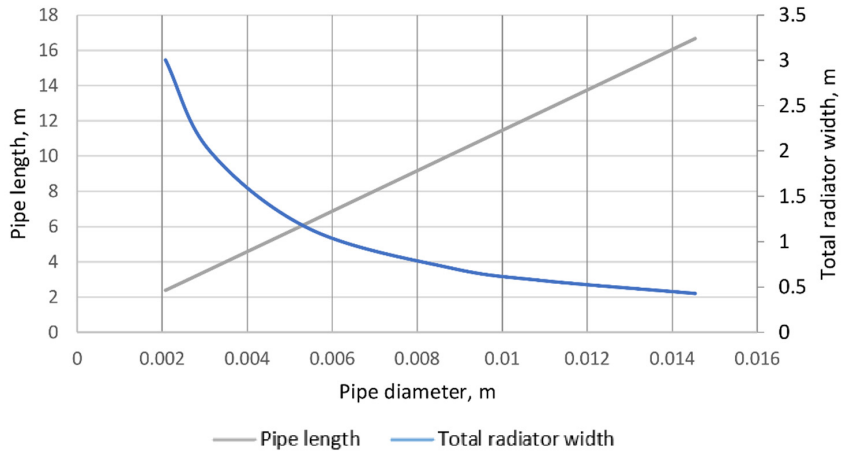

Figure 10. Dependence of the pipe length and the total width of the radiator on the pipe diameter (Refrigerant—NH_3).

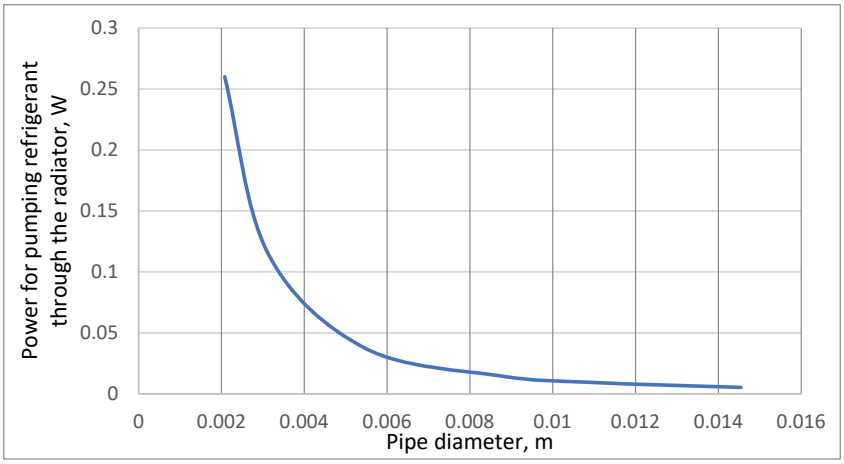

Figure 11. Dependence of the pumping power of the refrigerant through the radiator on the pipe diameter (Refrigerant—NH_3).

For a pipe with a diameter $d = 10.9$ mm at $Re = 4500$ ($B_R = 0.143\ m$), the following results were obtained:

Number of pipes: $n_p = 4$;

- Total width of radiator: $B_C = 0.56\ m$;
- Total width of the radiation surface: $B_{Ra} = 0.57\ m$;
- Pipe length: $L_R = 12.5\ m$;
- Power spent on pumping the refrigerant: $N_R = 0.0094\ W$.

For a pipe with a diameter $d = 5.5$ mm at $Re = 4500$ ($B_R = 0.143\ m$), the following results were obtained:

- Number of pipes: $n_p = 8$;
- Total width of radiator: $B_C = 0.138\ m$;
- Total width of the radiation surface: $B_{Ra} = 1.144\ m$;
- Pipe length: $L_R = 6.25\ m$;
- Power spent on pumping the refrigerant: $N_R = 0.038\ W$.

Analyzing the results, it can be seen that although the length of the pipe has decreased by 2 times, the power for pumping the refrigerant increased; however, the values remain insignificant.

The conducted studies show that when using liquid ammonia, there are more possibilities for varying the geometric parameters of the radiator and the power for pumping the refrigerant can be significantly reduced. The final decision related to the suitable radiator design can be made based on the operating conditions of the lunar power plant.

Next, the influence of the thermodynamic properties of the refrigerant on the main geometrical parameters of the radiator is studied using the previously derived formulas (53)–(66) for two refrigerants:

a. Helium;
b. Ammonia.

From the formula (55) for a flow with the same Re_m and given initial conditions $K_\mu = \frac{\mu_{v1}}{\mu_{v2}} = 9.49$; $K_h = \frac{\Delta h_{L1}}{\Delta h_{L2}} = 1.12$:

$$d_1 \cdot n_{p1} = \frac{K_\mu}{K_h} \cdot d_2 \cdot n_{p2} \tag{67}$$

If pipes of the same diameter are used, then:

$$n_{p1} = \frac{K_\mu}{K_h} \cdot n_{p2} \tag{68}$$

While using helium, the number of pipes n_{p1} will be 8.4 greater, compared to using liquid ammonia.

The fin width of the radiator during laminar flow ($\frac{Pe \cdot d}{L_R} < 100$; $Nu = 3.66$):

$$B_{R1} = K_\lambda \cdot B_{R2} \tag{69}$$

where the radiation surface ratio:

$$K_\lambda = \frac{\lambda_1}{\lambda_2} = 0.256 \tag{70}$$

The total heat transfer surface of the pipes:

$$S_{ta1} = \frac{S_{ta2}}{K_\lambda} \tag{71}$$

To reject the required heat from the FPSE using helium as a refrigerant, the total heat radiation surface area of the pipes will be 3.9 times larger, i.e., the specific heat flux emitted

by the pipe surface will be 3.9 times smaller, compared to using liquid ammonia. Therefore, the fin width is 3.9 times smaller when using helium, since less heat is radiated from the surface. Liquid ammonia allows the heat flux emitted by the radiator pipe section to increase. Therefore, it is possible to increase the width of the fin and reduce the length of the pipe. When using helium, the number of pipes and fin sections increases.

The results of the preliminary stage of calculation can be summed as follows. Taking into account the accepted assumptions, the total area of the radiator depends only on the temperature difference ($\Delta T = T_h - T_w$). If the difference is provided, then the area and the specific heat flux will be the same using any refrigerant. The thermodynamic properties affect the design parameters of the radiator (Pipe diameter d; number of pipes n_p; pipe length L_R, total radiator width B_a and the pumping power of the refrigerant through the radiator N_R).

It has been established that the use of liquid ammonia as a refrigerant makes it possible to reduce the power for pumping the refrigerant through the radiator. The formulas (67)–(71) can also be used to compare other refrigerants.

After performing the first stage of the enhanced calculation method, we move onto the next stage and perform calculations using the previously developed method (two-dimensional model). A comparative analysis for laminar (*Re* = 500) and turbulent (*Re* = 4500) flows for two refrigerants—helium and liquid ammonia—was carried out. The comparison results are presented in Tables 2–6 below.

Table 2. Comparative analysis for liquid ammonia (*Re* = 500; *d* = 0.002 m).

Parameter	Unit	2D Model	Enhanced Method	Deviation, %
Pipe length	m	1.821	1.8	1.15
Total area of the radiator	m^2	7.21	7.15	0.83
Power for pumping refrigerant through the radiator	W	0.0089	0.009	1.12

Table 3. Comparative analysis for liquid ammonia (*Re* = 4500; *d* = 0.0055 m).

Parameter	Unit	2D Model	Enhanced Method	Deviation, %
Pipe length	m	6.39	6.25	2.1
Total area of the radiator	m^2	7.28	7.11	2.3
Power for pumping refrigerant through the radiator	W	0.0371	0.038	2.4

Table 4. Comparative analysis for helium (*Re* = 500; *d* = 0.002 m).

Parameter	Unit	2D Model	Enhanced Method	Deviation, %
Pipe length	m	0.844	0.84	0.7
Total area of the radiator	m^2	7.2036	7.15	0.74
Power for pumping refrigerant through the radiator	W	5.09	5.08	0.27

Table 5. Comparative analysis for helium (*Re* = 4500; *d* = 0.002 m).

Parameter	Unit	2D Model	Enhanced Method	Deviation, %
Pipe length	m	1.473	1.46	0.88
Total area of the radiator	m^2	7.2242	7.15	1.03
Power for pumping refrigerant through the radiator	W	217.3795	222.6	2.4

Table 6. Comparative analysis for helium (Re = 4500; d = 0.0102 m).

Parameter	Unit	2D Model	Enhanced Method	Deviation, %
Pipe length	m	7.9	7.83	0.9
Total area of the radiator	m^2	6.37	6.3	1
Power for pumping refrigerant through the radiator	W	7.37	7.7	4.4

The results of calculations using the previously developed two-dimensional radiator model by the authors confirmed the acceptable accuracy of the results obtained at the preliminary stage of the enhanced method presented in this work.

When considering a laminar flow (Re = 500), the maximum deviation in the radiator area is 0.83%, N_R—1.12%. For turbulent flows (Re = 4500), the error increases:

- For liquid ammonia:
  - Total area of the radiator—2.3%;
  - N_R—2.4%.
- For helium:
  - Total area of the radiator—1.0%;
  - N_R—4.4%

The conducted studies proved the effectiveness of the preliminary calculations using the derived formulas presented in this work. The enhanced method made it possible to effectively evaluate the capabilities of various refrigerants and choose the main design radiator parameters and the refrigerant flow regime in a less time-consuming process and with minimal deviations (<5%), compared to the previously developed two-dimensional radiator model by the authors.

4. Conclusions

Thermal management plays a major role in determining the success of space missions. This work presents an enhanced calculation method for a radiator of the heat rejection system of the FPSE designed to operate on the Moon. The enhanced calculation method allows less time for determining the main design parameters of the radiator and the most effective refrigerant compared to a previously developed calculation method by the authors. The major highlights and conclusions of this work are summarized as follows:

1. The enhanced method was validated by a comparative analysis using helium or liquid ammonia as a refrigerant in the heat rejection system of the FPSE designed to operate on the Moon within the temperature range of 260–280 K.
2. The dependences of the change in the geometrical parameters of the radiator on the thermodynamic properties of the refrigerant and the flow regime were established.
3. An example of selecting the dimensions of a radiator with a given specific radiation flux per unit area using helium and liquid ammonia was presented.
4. It has been established that when using liquid ammonia, there are more possibilities for varying the geometric parameters of the radiator. The use of liquid ammonia as a refrigerant makes it possible to:
   - Reduce the power spent pumping the refrigerant through the radiator. For helium, even with an increase in pipe diameter to d = 10.8 mm with a turbulent flow Re = 4500, the power for pumping the refrigerant was $N_R = 5.1$ W; on the other hand, while using liquid ammonia $N_R = 0.27$ W.
   - Increase the heat flow per unit area of the radiator pipe by 3.9 times, which allows the fin width to be increased and reduces the length of the radiator pipe.
5. The conducted studies proved the effectiveness of the preliminary calculations using the derived formulas presented in this work. The enhanced method made it possible to effectively evaluate the capabilities of various refrigerants and choose the radiator

parameters and the refrigerant flow regime in a less time-consuming process and with minimal deviations (<5%) compared to the previously developed two-dimensional radiator model by the authors. The largest deviations were noted for turbulent flows (Re = 4500):

For liquid ammonia:

- Total area of the radiator—2.3%;
- N_R—2.4%.

For helium:

- Total area of the radiator—1.0%;
- N_R—4.4%.

Author Contributions: Conceptualization, S.S. and Y.A.; Formal analysis, S.S. and H.K.; Investigation, S.S., Y.A. and H.K.; Methodology, S.S. and Y.A.; Supervision, S.S., M.S. and I.T.; Validation, M.S., Y.A. and I.T.; Visualization, H.K.; Writing—original draft, S.S. and Y.A.; Writing—review and editing, S.K. and H.K. All authors have read and agreed to the published version of the manuscript.

Funding: This research received no external funding.

Institutional Review Board Statement: Not applicable.

Informed Consent Statement: Not applicable.

Data Availability Statement: Not applicable.

Acknowledgments: This paper has been supported by the RUDN University Strategic Academic Leadership Program.

Conflicts of Interest: The authors declare no conflict of interest.

Nomenclature

q_{rad}	Amount of heat released due to radiation, J
q_{conv}	Amount of heat released due to convection, J
q_L	Amount of heat that must be rejected from the refrigerant through one pipe, J
q_s	Amount of heat that must be rejected from the radiator, J
n_p	The number of radiator pipes required for the heat rejection process
Δh_L	Change in stagnation enthalpy through one pipe, J
Δh	Change in specific enthalpy through one pipe, J/kg
G_s	Refrigerant mass flow rate through radiator, kg/s
h_{in}	Stagnation enthalpy at the inlet, J
h_{out}	Stagnation enthalpy at the outlet, J
G_{ref}	Refrigerant mass flow rate through one pipe, kg/s
ρ_{in}	Refrigerant density at the pipe inlet, $\frac{\text{kg}}{m^3}$
w_{in}	Refrigerant flow speed at the pipe inlet, m/s
d	The inner diameter of the radiator pipe, m
α	Heat transfer coefficient, $\frac{W}{m^2 \cdot K}$
S_t	Surface area for heat transfer, m^2
T_h	Refrigerant temperature, K
T_m	Refrigerant mean temperature, K
T_w	Pipe wall temperature, K
L_R	Pipe length, m
q_R	Heat flux as a result of radiation, W
σ	Stefan–Boltzmann constant, $\frac{W}{m^2 \cdot K^4}$
ε	Emissivity coefficient
F_R	Radiator radiation area, m^2
T_S	Ambient temperature, K
B_R	Fin width, m
T_R	Fin surface temperature, K

F_{Ramin}	The minimum total area of radiator radiation for heat rejection of a given heat flux, m^2
q_{Fmax}	Maximum heat flux per unit area of radiator radiation, J
F_{Ra}	Total radiator radiation area, m^2
B_{Ra}	Total width of the radiation surface of the radiator, m
Re_m	Mean value of Reynolds
Re_{in}	Reynolds number at the inlet
μ_{in}	Refrigerant dynamic viscosity at the inlet, Pa.s
μ_{out}	Refrigerant dynamic viscosity at the outlet, Pa.s
ν_{in}	Refrigerant kinematic viscosity at the inlet, $\frac{m^2}{s}$
μ_v	Viscosity coefficient
A_1	Coefficient for convenience
K_T	Coefficient of temperature difference during convective heat exchange between the refrigerant and the pipe wall
B_S	Distance between two pipes' centers, m
t	Pipe wall thickness, m
b_{r1}	Fin width (related to a specific design option), m
h_R	Fin thickness, m
q_F	Specific heat flux per unit area of radiator surface, J/m^2
N_R	The power spent on pumping the refrigerant through the radiator, W
ΔP_R	Pressure drop due to friction in the radiator pipes, Pa
ρ_h	Refrigerant density in the radiator, $\frac{kg}{m^3}$
η	Efficiency of the refrigerant pump
f	Friction factor
w_h	Refrigerant velocity, m/s
ν_m	Refrigerant mean kinematic viscosity, $\frac{m^2}{s}$
A_{N_R}	Pumping power coefficient
Nu	Nusselt number
λ	Refrigerant thermal conductivity, $\frac{W}{m \cdot K}$
Re	Reynolds number
Pe	Peclet number
Pr	Prandtl Number
a	Thermal diffusivity, m^2/s
γ	Kinematic viscosity, m^2/s
K_μ	Viscosity ratio of the two refrigerants
K_h	Enthalpy ratio of the two refrigerants
K_λ	Radiation surface ratio of the two refrigerants
S_{ta}	Total required radiation surface, m^2
B_C	Total width of radiator, m

Appendix A Calculation of the Width of the Radiator Radiation Surface

Each radiator pipe has two fins for radiating heat into free space: one from the left side, and another from the right side. The fins are symmetric with respect to the pipe. When calculating the width of the radiator's radiation surface, two options were considered (Figures A1 and A3).

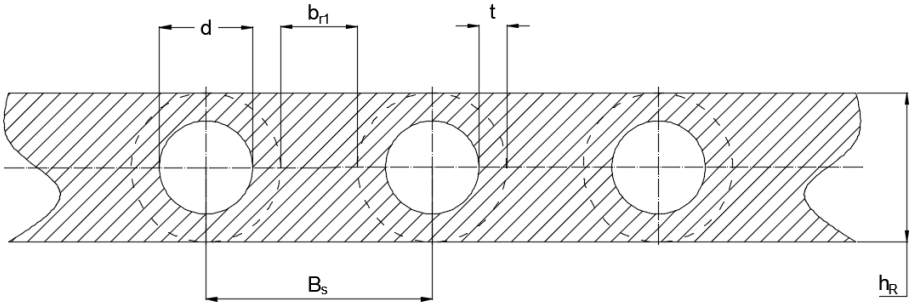

Figure A1. Radiator design (option 1).

The radiation surface width was calculated as follows:

$$B_S = B_R = d + 2t + b_{r1} \tag{A1}$$

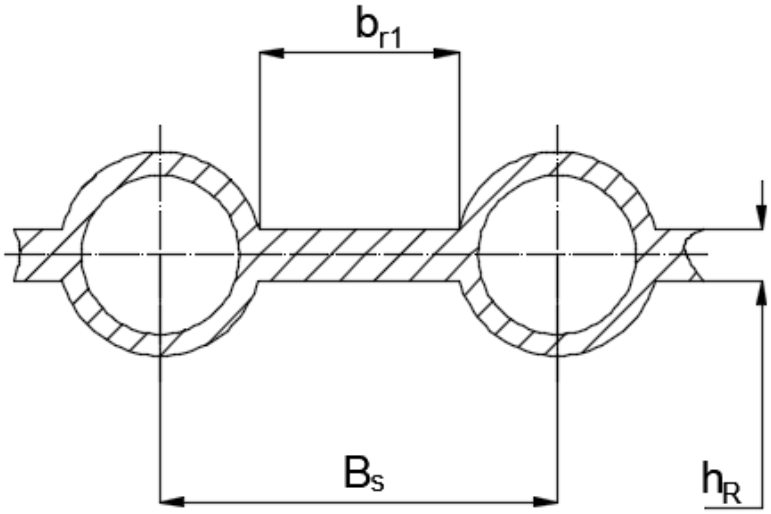

(**a**)

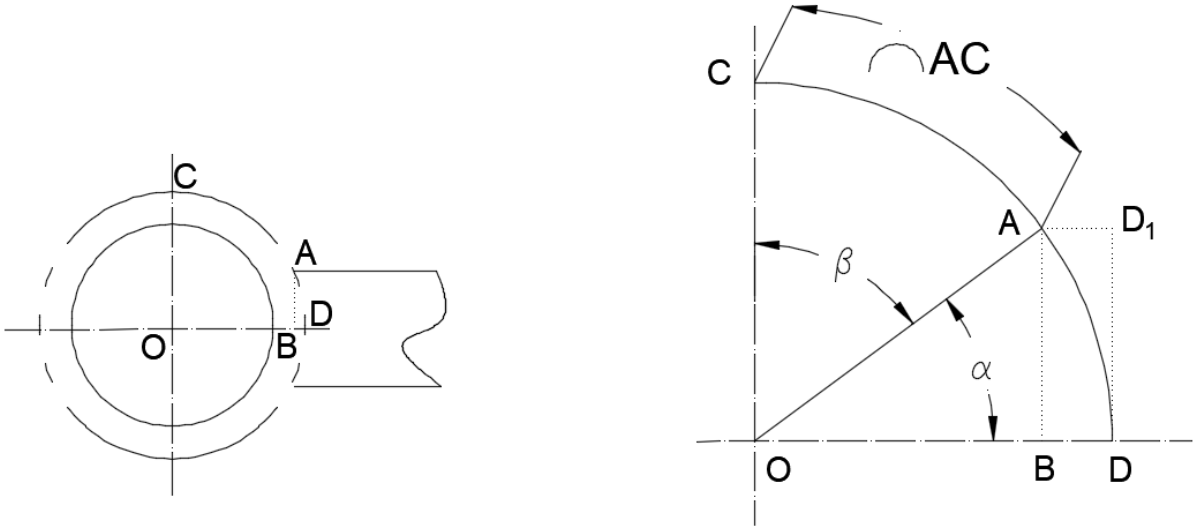

(**b**)

Figure A2. (**a**) Radiator design (option 2); (**b**) Calculation of radiator design (option 2).

For option 2, the radiation surface width was calculated as follows:

$$B_R = b_{r1} + 2(|AD_1| + |AC|) \tag{A2}$$

where

$$B_S = b_{r1} + 2|OD| \tag{A3}$$

$$\frac{|AC|}{\pi(d+2t)} = \frac{\beta}{2\pi} \tag{A4}$$

$$|AC| = \frac{d+2t}{2}\beta \tag{A5}$$

$$\alpha = arcsin\left(\frac{h_R}{d+2t}\right) \tag{A6}$$

$$\beta = \frac{\pi}{2} - \alpha \tag{A7}$$

$$|OD| = \frac{d}{2} + t \tag{A8}$$

$$|AD_1| = |BD| = |OD| - |OB| = \left(\frac{d}{2} + t\right) - \left(\frac{d}{2} + t\right)cos\alpha = \left(\frac{d}{2} + t\right)(1 - cos\alpha) \tag{A9}$$

Rearranging them, the following formulas are obtained:

$$B_R = b_{r1} + (d + 2t)[(1 - cos\alpha) + \beta] \tag{A10}$$

$$B_S = b_{r1} + d + 2t \tag{A11}$$

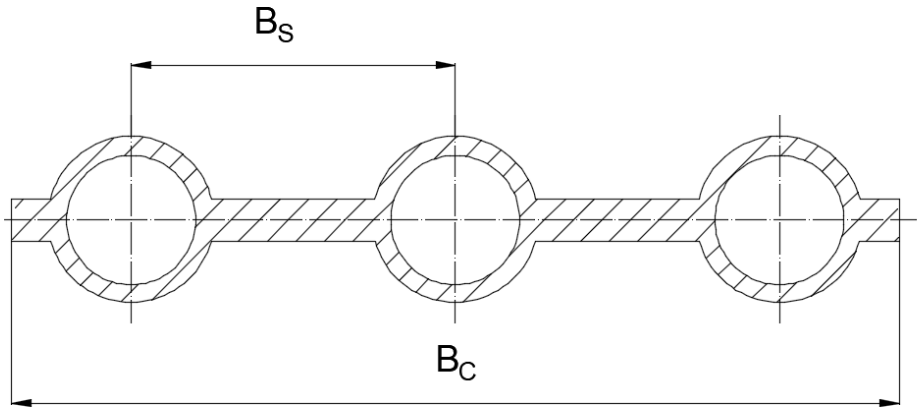

Figure A3. Total dimensions of the radiator (option 2).

The total width of the radiator was calculated as follows:

$$B_C = B_S \cdot n_p \tag{A12}$$

For option 2, the total width of the radiation surface of the radiator B_{Ra} and the total width of the radiator B_C ($B_{Ra} > B_C$) are different.

When using option 2 with protruding pipes' radiation surfaces, it must be taken into account that the amount of heat determined by the Stefan–Boltzmann law is reflected in different directions. The change in radiation in individual directions is determined by Lambert's law, which is strictly defined for a completely black body. For rough bodies, this law is confirmed only for angles of deviation from the normal to the radiation surface up to 60° [30]. Lambert's law is used to calculate radiant heat transfer between surfaces of finite dimensions. The scheme of option 2 shown in Figure A4 is simplified. From protruding surfaces, radiation can reach the surface of the fins (a–b) and adjacent radiator pipes (b–c).

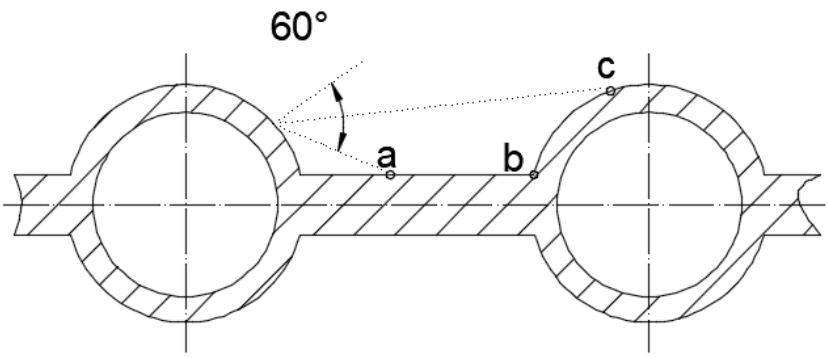

Figure A4. Radiation from the surface of the radiator (option 2).

To avoid such situations in a real design, it is necessary to perform special smooth transitions (fillets) from the fin to the pipe as shown in Figure A5.

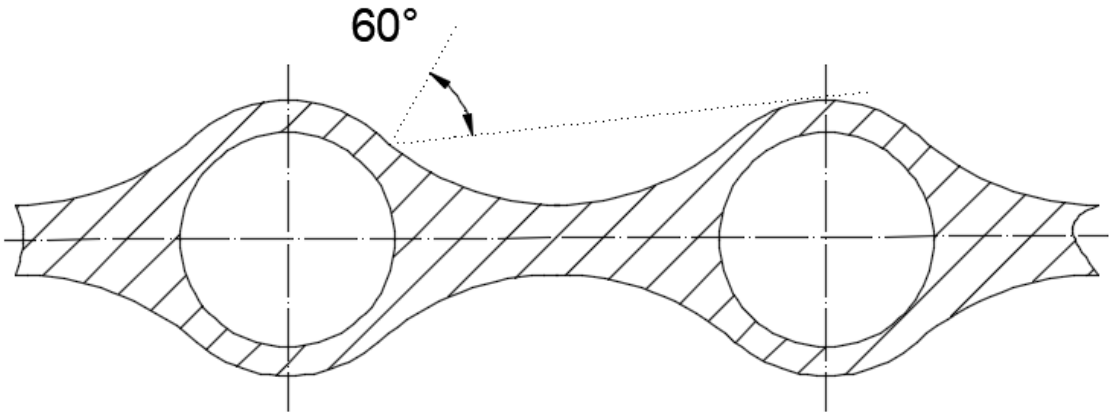

Figure A5. Radiation from the enhanced surface of the radiator (option 2).

References

1. Russia and China Team Up to Build a Moon Base | Science | The Guardian. Available online: https://www.theguardian.com/science/2021/jun/25/russia-china-team-up-build-moon-base (accessed on 20 January 2022).
2. NASA's Artemis Base Camp on the Moon Will Need Light, Water, Elevation | NASA. Available online: https://www.nasa.gov/feature/goddard/2021/nasa-s-artemis-base-camp-on-the-moon-will-need-light-water-elevation (accessed on 20 January 2022).
3. ESA—Future Moon Base. Available online: https://www.esa.int/ESA_Multimedia/Images/2018/11/Future_Moon_base (accessed on 20 January 2022).
4. Stirling Convertor Sets 14-Year Continuous Operation Milestone | NASA. Available online: https://www.nasa.gov/feature/glenn/2020/stirling-convertor-sets-14-year-continuous-operation-milestone (accessed on 20 January 2022).
5. Heat Rejection Technologies for Nuclear Systems | NASA SBIR & STTR Program Homepage. Available online: https://sbir.nasa.gov/content/heat-rejection-technologies-nuclear-systems (accessed on 2 March 2022).
6. Iwata, N.; Nakanoya, S.; Nakamura, N.; Takeda, N.; Tsutsui, F. Thermal Performance Evaluation of Space Radiator for Single-Phase Mechanically Pumped Fluid Loop. *J. Spacecr. Rockets* **2022**, *59*, 225–235. [CrossRef]
7. Paris, A.D.; Bhandari, P.; Birur, G.C. High Temperature Mechanically Pumped Fluid Loop for Space Applications -Working Fluid Selection. *SAE Tech. Pap.* **2004**, *113*, 892–898.
8. Van Es, J.; van den Berg, T.; van Vliet, A.; Ganzeboom, T.; Brouwer, H.; Elvik, S. Mini Mechanically Pumped Loop Modelling and Design for Standardized CubeSat Thermal Control. In Proceedings of the 50th International Conference on Environmental Systems (ICES 2021), Lisbon, Portugal, 12–15 July 2021.
9. Wang, J.X.; Li, Y.Z.; Zhang, Y.; Li, J.X.; Mao, Y.F.; Ning, X.W. A Hybrid Cooling System Combining Self-Adaptive Single-Phase Mechanically Pumped Fluid Loop and Gravity-Immune Two-Phase Spray Module. *Energy Convers. Manag.* **2018**, *176*, 194–208. [CrossRef]
10. Wang, J.X.; Li, Y.Z.; Zhang, H.S.; Wang, S.N.; Liang, Y.H.; Guo, W.; Liu, Y.; Tian, S.P. A Highly Self-Adaptive Cold Plate for the Single-Phase Mechanically Pumped Fluid Loop for Spacecraft Thermal Management. *Energy Convers. Manag.* **2016**, *111*, 57–66. [CrossRef]
11. Lee, K.-L.; Li, Y.; Guzek, B.J.; Kadambi, J.R.; Kamotani, Y. Compact Heat Rejection System Utilizing Integral Variable Conductance Planar Heat Pipe Radiator for Space Application. *Gravitational Sp. Res.* **2015**, *3*, 30–41. [CrossRef]
12. Lee, K.L.; Tarau, C.; Anderson, W.G.; Beard, D. Titanium-Water Heat Pipe Radiators for Space Fission Power System Thermal Management. *Microgravity Sci. Technol.* **2020**, *32*, 453–464. [CrossRef]
13. Lin, M.; Mou, J.; Chi, C.; Hong, G.; Ge, P.; Hu, G. A Space Power System of Free Piston Stirling Generator Based on Potassium Heat Pipe. *Front. Energy* **2020**, *14*, 1–10. [CrossRef]
14. Tarau, C.; Anderson, W.G.; Miller, W.O.; Ramirez, R. Sodium VCHP with Carbon-Carbon Radiator for Radioisotope Stirling Systems. *AIP Conf. Proc.* **2010**, *1208*, 42–54.
15. Anderson, W.G.; Tarau, C. Variable Conductance Heat Pipes for Radioisotope Stirling Systems. *AIP Conf. Proc.* **2008**, *969*, 679–688.
16. Hertzberg, A. Thermal Management in Space. Available online: https://space.nss.org/settlement/nasa/spaceresvol2/thermalmanagement.html (accessed on 21 January 2021).
17. Antipov, Y.A.; Smirnov, S.V.; Oshchepkov, P.P.; Khalife, H.S. Design Features of a Power Plant Based on a Stirling Engine Working on the Moon. *Adv. Astronaut. Sci.* **2021**, *174*, 833–847.
18. Badger, B. Ammonia: The Refrigerant of the Future. Available online: https://www.energy-learning.com/index.php/opinion/112-ammonia-the-refrigerant-of-the-future (accessed on 21 January 2021).

19. Smirnov, S.V.; Sinkevich, M.V.; Antipov, Y.A.; Khalife, H.S. A Calculation Method of a Heat Rejection System in a Lunar Power Plant Consisting of a Free-Piston Stirling Engine (FPSE). *Acta Astronaut.* **2021**, *180*, 46–57. [CrossRef]
20. Microgen Engine Corporation—Microgen. Available online: https://www.microgen-engine.com/ (accessed on 5 February 2022).
21. Evogress—Innovative Power Generation Technologies. Available online: http://www.evogress.com/en/ (accessed on 5 February 2022).
22. Ivanov, V.L.; Fisher, Y.V.; Korniychuk, S.P.; Kisilev, N.A. Space Radiant Heat Exchanger for Heat Elimination. *Sci. Educ.* **2011**, *10*, 12.
23. Hesselgreaves, R.E.; Law, D.R. *Compact Heat Exchangers*; Butterworth-Heinemann: Oxford, UK, 2016.
24. Tsvetkov, F.F. *Problem Book in Heat and Mass Transfer*; Publishing House MEI: Moscow, Russia, 2008.
25. Petukhova, B.S.; Shilkov, V.K. *Handbook of Heat Exchangers*; Energoatomizdat: Moscow, Russia, 1987.
26. Williams, J.P.; Paige, D.A.; Greenhagen, B.T.; Sefton-Nash, E. The Global Surface Temperatures of the Moon as Measured by the Diviner Lunar Radiometer Experiment. *Icarus* **2017**, *283*, 300–325. [CrossRef]
27. What Is the Temperature on the Moon? | Space. Available online: https://www.space.com/18175-moon-temperature.html (accessed on 12 June 2021).
28. Golubev, I.F.; Kiyashova, V.P. *Thermophysical Properties of Ammonia*; Publishing House of Standards: Moscow, Russia, 1978.
29. Thermophysical Properties of Fluid Systems. Available online: https://webbook.nist.gov/chemistry/fluid/ (accessed on 12 June 2021).
30. Mikheev, M.A.; Mikheeva, I.M. *Basics of Heat Transfer*; Energia: Moscow, Russia, 1977.